Bioconjugate Chemistry

Article

pubs.acs.org/bc

Site-Specific Labeling of Cysteine-Tagged Camelid Single-Domain Antibody-Fragments for Use in Molecular Imaging

Sam Massa,[†,‡,§] Catarina Xavier,[†] Jens De Vos,[†,‡,§] Vicky Caveliers,[†,⊥] Tony Lahoutte,[†,⊥] Serge Muyldermans,[‡,§] and Nick Devoogdt*[,†,‡]

[†]In Vivo Cellular and Molecular Imaging Laboratory, Vrije Universiteit Brussel (VUB), 1090 Brussels, Belgium

[‡]Laboratory of Cellular and Molecular Immunology, Vrije Universiteit Brussel (VUB), 1050 Brussels, Belgium

[§]VIB Structural Biology Research Center, Vrije Universiteit Brussel (VUB), 1050 Brussels, Belgium

[⊥]Nuclear Medicine Department, Universitair Ziekenhuis Brussel, Vrije Universiteit Brussel (VUB), 1090 Brussels, Belgium

Supporting Information

ABSTRACT: Site-specific labeling of molecular imaging probes allows the development of a homogeneous tracer population. The resulting batch-to-batch reproducible pharmacokinetic and pharmacodynamic properties are of great importance for clinical translation. Camelid single-domain antibody-fragments (sdAbs)—the recombinantly produced antigen-binding domains of heavy-chain antibodies, also called Nanobodies—are proficient probes for molecular imaging. To safeguard their intrinsically high binding specificity and affinity and to ensure the tracer's homogeneity, we developed a generic strategy for the site-specific labeling of sdAbs via a thio-ether bond. The unpaired cysteine was introduced at the carboxyl-terminal end of the sdAb to eliminate the risk of antigen binding interference. The spontaneous dimerization and capping of the unpaired cysteine required a reduction step prior to conjugation. This was optimized with the mild reducing agent 2-mercaptoethylamine in order to preserve the domain's stability. As a proof-of-concept the reduced probe was subsequently conjugated to maleimide-DTPA, for labeling with indium-111. A single conjugated tracer was obtained and confirmed via mass spectrometry. The specificity and affinity of the new sdAb-based imaging probe was validated in a mouse xenograft tumor model using a modified clinical lead compound targeting the human epidermal growth factor receptor 2 (HER2) cancer biomarker. These data provide a versatile and standardized strategy for the site-specific labeling of sdAbs. The conjugation to the unpaired cysteine results in the production of a homogeneous group of tracers and is a multimodal alternative to the technetium-99m labeling of sdAbs.

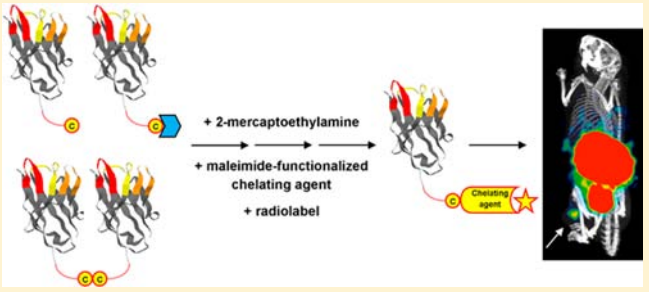

INTRODUCTION

Antibodies and antibody-derived fragments are widely used targeting probes in molecular imaging and therapy. Their derivatization involves conjugation of a bifunctional ligand, label, or drug to a functional group present on their surface. Generally the primary amines of lysines or the sulfhydryls of cysteines serve as conjugation sites. Conjugation to lysines is an obvious choice due to their abundant occurrence and accessibility, but also entails disadvantages. Because of the presence of several solvent exposed lysines, this conjugation strategy yields a heterogeneous mixture of probes labeled to various extents, at different positions,[1] and is therefore considered random. Moreover, conjugation to lysines in or near the antigen-binding site may lead to steric hindrance of target recognition. The latter problem is circumvented by the derivatization on cysteines. This amino acid is less abundant and forms conserved disulfide bridges in antibodies. Preferential reduction of interchain disulfide bonds is possible, but still results in heterogeneous antibody-conjugates.[2] Characterization of heterogeneous tracer populations remains a major issue, since the number and position of labels/drugs affect the biodistribution profile in the organism and the therapeutic index of the conjugate.[3−5] Such pharmacokinetic and pharmacodynamic differences pose an important challenge in the clinical translation of antibody-derived conjugates in terms of manufacturing and characterization, as well as in achieving market approval. In order to obtain a homogeneous tracer population with a fixed conjugation at a specific location, the introduction of an additional, unpaired cysteine offers a valuable alternative.[6−8] An introduced unpaired cysteine forms a unique place for conjugation. We aim to apply this strategy for the site-specific labeling of camelid single-domain antibody-fragments (sdAbs).

A sdAb, also known as Nanobody or V_HH, is the autonomous antigen-binding domain of heavy-chain-only antibodies, occurring in species of the family of Camelidae.[9]

Received: March 16, 2014
Revised: April 21, 2014
Published: April 24, 2014

   dx.doi.org/10.1021/bc500111t | *Bioconjugate Chem.* 2014, 25, 979−988

Scheme 1. Schematic Overview of the sdAb Constructs and Strategies for Labeling[a]

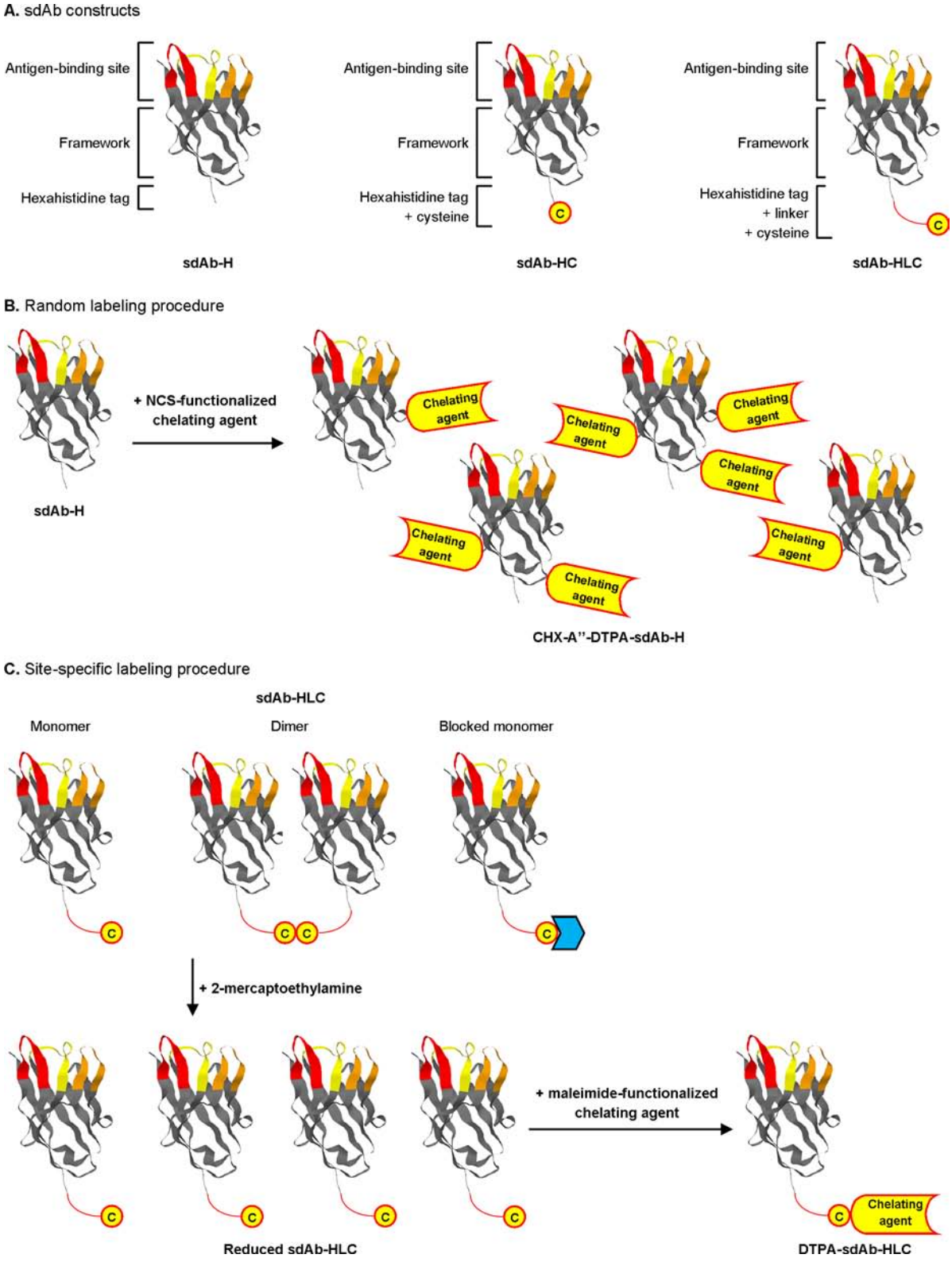

[a](A) Illustration of the used sdAb constructs, based on the *in silico* predicted structure of sdAb 2Rs15d.[24] (B) Random labeling procedure for sdAb-H constructs. Positions of the chelating agents are shown fictively. Other combinations with 1 and 2 chelating agents are possible. (C) Site-specific labeling procedure for sdAb-HLC constructs, with intermediate reduction step with 2-MEA.

Due to their small size (15 kDa), high stability, and specificity for their target, sdAbs have found their way into many applications and were shown to be proficient in the field of molecular imaging.[10,11] Indeed, radiolabeled sdAbs target their antigen efficiently *in vivo* and are cleared rapidly from the body, hereby generating highly specific contrast images at early time

dx.doi.org/10.1021/bc500111t | *Bioconjugate Chem.* 2014, 25, 979−988

points after injection.[12] Currently, sdAb 2Rs15d, targeting human epidermal growth factor receptor 2 (HER2), has entered a phase 1 clinical trial in HER2-positive breast cancer patients. This sdAb was selected as lead compound based on its high production yields, target affinity, tumor uptake, and tumor-to-background ratios in HER2-positive xenografted mice after ^{99m}Tc-tricarbonyl complexation of the carboxyl-terminal hexahistidine tag.[13] Moreover, sdAb 2Rs15d was also selected for the absence of lysines in its antigen-binding loops, leading to a successful conjugation of NOTA to lysines for labeling with ^{68}Ga without compromising the antigen-binding capacity.[14] However, this random labeling strategy still yields a heterogeneous mixture of sdAbs conjugated to 0, 1, and 2 NOTA's. The development of a site-specific labeling procedure of sdAbs is thus important to enter the clinic more easily in the future. Furthermore, a generic strategy for site-specific labeling of sdAbs is of high interest, since other imaging tracers are currently also under development [in the field of oncology: CEA,[15] EGFR,[16] multiple myeloma;[17] cardiovascular diseases: VCAM1,[18] Lox1;[19] inflammation: MMR,[20,21] VSIG4[22]].

To site-specifically label sdAbs via a thio-ether bond we investigated the use of a sdAb construct with an unpaired cysteine. The cysteine was introduced at the sdAb carboxyl terminus, positioning the conjugation-site on the opposite side of the antigen-binding region to avoid antigen binding interference.[23] This unpaired cysteine oxidized spontaneously into sdAb dimers, which necessitated an optimized reduction step prior to conjugation with a maleimide-functionalized chelating agent. The conjugate was then labeled and its stability was characterized. The functionality of the new tracer was validated *in vitro* and *in vivo* in a HER2 xenograft mouse model. In this preclinical proof-of-concept we chose to employ the bifunctional ligand maleimide-DTPA in combination with ^{111}In for use in single-photon emission computed tomography (SPECT). The strategy is nevertheless generic since it should work with any maleimide-functionalized chelating agent or label in any modality.

RESULTS

Design and Expression of a sdAb Construct with an Unpaired Cysteine. A generic strategy for site-specific labeling of sdAbs was developed using the anti-HER2 sdAb 2Rs15d and the nontargeting control sdAb BcII10 as model compounds. To perform site-specific conjugation via a thio-ether bond we cloned the sdAbs in a plasmid with a carboxyl-terminal unpaired cysteine after the hexahistidine tag (sdAb-HC) (Scheme 1A). Bacterial expression and purification from a periplasmic extract using affinity chromatography and subsequent size-exclusion chromatography (SEC) showed, however, that production yields dropped to 5% or less of production yields of the original sdAb constructs without cysteine after the hexahistidine tag (sdAb-H) (Table 1). This drop in production yield was consistent for several other sdAbs as well (data not shown). Together with a high variability in turbidity of the culture after overnight expression, presence of the sdAb in the culture medium, and a viscous periplasmic extract, these observations indicated a possible and variable level of cell lysis and toxicity for the bacterial host of the sdAb construct with carboxyl-terminal unpaired cysteine.

Since the unpaired cysteine might be interfering with the correct folding of the internal disulfide bond present in the sdAb, we chose to reclone the sdAbs into a plasmid in which the cysteine is spaced by a linker from the sdAb sequence. In the construct sdAb-HLC the cysteine is spaced from the sdAb by a rigid linker consisting of the 14 amino acids SPSTPPTPSPSTPP (Scheme 1A), derived from the hinge sequence of a human IgA1. The disturbance in bacterial expression of sdAbs with an unpaired cysteine is less pronounced for this construct and the production yield approaches that of original unmodified sdAb-H (Table 1). We therefore continued with the sdAb-HLC constructs.

Table 1. Carboxyl-Terminal Cysteine-Tagged Construct sdAb-HLC, in which a Rigid Linker Separates the Cysteine from the sdAb, Showed a Higher Production Yield in a Bacterial Expression System in Comparison to the Construct sdAb-HC where the Cysteine Comes Immediately after the Hexahistidine Tag[a]

sdAb	construct	production yield (mg/L culture)	% of sdAb-H production yield
2Rs15d	H	2.46	
	HC	0.05	2%
	HLC	1.15	47%
BcII10	H	5.10	
	HC	0.28	5%
	HLC	4.13	81%

[a]The production yield of the hexahistidine-tagged construct sdAb-H is given as a reference. Production yields were determined after subsequent affinity and size exclusion chromatography purification from bacterial periplasmic extracts.

Reduction and Conjugation. In the final purification step, sdAb-HLC eluted from SEC in two peaks (Figure S1A, Supporting Information). Nonreducing and reducing lithium dodecylsulfate polyacrylamide gel electrophoresis (LDS-PAGE) showed that the first peak consisted of disulfide-linked dimeric sdAb, whereas the second peak consisted of monomeric sdAb (Figure S1B, Supporting Information). Additional electrospray ionization quadrupole time-of-flight (ESI-Q-ToF) mass spectrometry characterization confirmed these results, but showed that the second peak, besides monomeric sdAb-HLC with an unpaired cysteine, also contained sdAb-HLC bound to a molecule of 306 Da (Figure S2, Supporting Information). The presence of spontaneously dimerized sdAb-HLC and blocked monomeric sdAb-HLC required the introduction of a reduction step prior to conjugation with a maleimide-functionalized chelating agent, to maximize the available amount of sdAbs for site-specific conjugation (Scheme 1C).

For the reduction reaction the mild reducing agent 2-mercaptoethylamine (2-MEA) was selected in order to preserve the intradomain disulfide bridges, which are crucial for the stability of a sdAb. Reduction of sdAb-HLC (at a final concentration of 1 mg/mL) with a 180-fold molar excess of 2-MEA in PBS (pH 7.4) for 90 min at 37 °C was found optimal. The subsequent reaction with a 10-fold molar excess of bifunctional ligand maleimide-DTPA in 0.2 M NH_4OAc (pH 6.0) resulted in a successful site-specific conjugation. An additional SEC purification step was introduced to remove the remaining mixed-disulfide reduction intermediate sdAb-2-MEA and excess of bifunctional ligand, to end with a chemically defined conjugate of 1 sdAb bound to 1 chelating agent (Figure 1).

Radiolabeling and Stability. After site-specific conjugation with maleimide-DTPA, the sdAb was radiolabeled with ^{111}In and further characterized. The derivatized sdAbs were labeled at a final concentration of 10^{-5} M with activities ranging

dx.doi.org/10.1021/bc500111t | *Bioconjugate Chem.* 2014, 25, 979−988

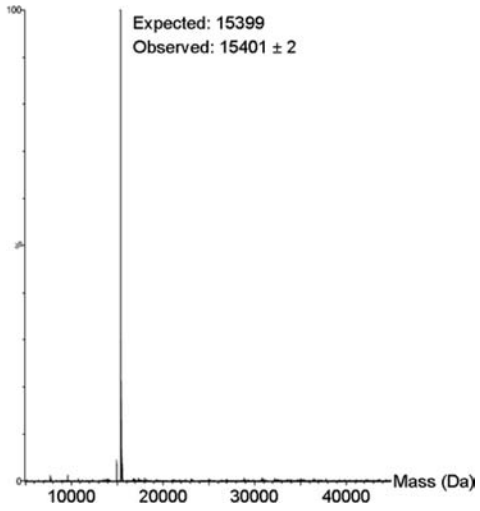

Figure 1. Single-conjugated sdAb was obtained after the site-specific conjugation procedure. ESI-Q-ToF mass spectrometry analysis identified a single peak of 15 401 Da, corresponding to the site-specific conjugation of one maleimide-DTPA to sdAb 2Rs15d-HLC (expected mass: 15 399 Da).

from 14.8 to 177.6 MBq. The variation in starting activity did not affect the labeling yield. After 30 min incubation at room temperature, the radiochemical purity was determined to be 94.0% ± 4.9% by instant thin-layer chromatography (iTLC). Increasing the incubation temperature of the labeling reaction resulted in increased labeling efficiencies with purities of 94.9% ± 1.7% at 37 °C and 97.0% ± 0.5% at 50 °C. The latter temperature was used for further labeling reactions. After additional gel-filtration chromatography the final radiochemical purity was 97.9% ± 0.6%. Alternatively, reverse-phase HPLC (RP-HPLC) analysis showed a radiochemical purity of 97.6% ± 1.9% (Figure 2A). The specific activity of the purified radiolabeled sdAb ranged from 9 to 49 MBq/nmol.

The stability of the radiolabeled sdAb conjugate was tested in PBS (pH 7.4). After 3 h the radiochemical purity was still 96.8% ± 0.6%, as determined by iTLC. Furthermore, the radiolabeled conjugate showed to be stable in human blood plasma. After incubation for 90 min at 37 °C, which corresponds to the early time point for *in vivo* sdAb biodistribution analyses, SEC analysis showed that 97.0% ± 2.5% of the radioactivity corresponded to the sdAb conjugate (Figure 2B). After 24 h incubation the radiochemical purity was still 92.9% ± 1.7%.

***In Vitro* Characterization.** The binding affinity of the sdAb 2Rs15d-HLC was determined on immobilized recombinant HER2 protein by surface plasmon resonance. The sdAb was still able to bind the recombinant protein after each step in the site-specific labeling process: reduction with 2MEA, conjugation to maleimide-DTPA, and (cold) labeling with indium (Table 2). The dissociation equilibrium constant of the site-specific conjugated sdAb DTPA-2Rs15d-HLC was determined to be 5.9 nM, compared to 5.1 nM for the original construct that was randomly conjugated on the lysines (CHX-A″-DTPA-2Rs15d-H). The kinetic parameters were thus retained after the site-specific conjugation process (Table 2).

Besides on recombinant protein, the functionality of the sdAb DTPA-2Rs15d-HLC was also tested on HER2-positive SKOV3 cells after radiolabeling with ^{111}In. Specific binding could be demonstrated by coincubation with a 1000-fold molar

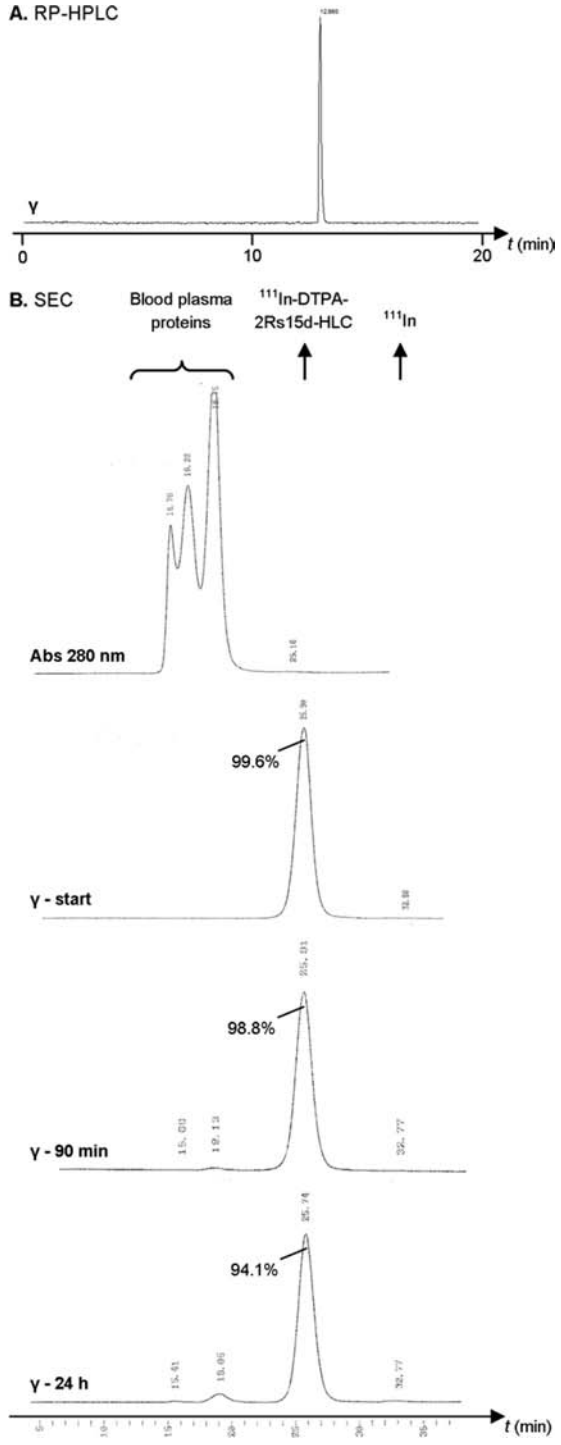

Figure 2. Radiolabeled sdAb complex ^{111}In-DTPA-2Rs15d-HLC showed high radiochemical purity and was stable in human blood plasma at 37 °C. (A) The radiochemical purity after the labeling and purification procedure was analyzed via RP-HPLC. The γ-spectrum chromatogram of a representative experiment is shown (^{111}In-DTPA-2Rs15d-HLC: 13.0 min). (B) ^{111}In-DTPA-2Rs15d-HLC was incubated in human blood plasma at 37 °C. The 280 nm absorbance chromatogram (at the start of incubation) and the γ-spectrum chromatograms (at the start of incubation and after 90 min and 24 h of incubation) of the SEC elution profile are shown from a representative experiment. Human blood plasma proteins (14.8−18.8 min), ^{111}In-DTPA-2Rs15d-HLC (25.9 min), and free ^{111}In (32.8 min) are indicated, as well as the % area-under-the-curve for ^{111}In-DTPA-2Rs15d-HLC.

dx.doi.org/10.1021/bc500111t | *Bioconjugate Chem.* 2014, 25, 979−988

Table 2. SdAb Construct 2Rs15d-HLC Retained Its Binding Affinity after Every Step of the Site-Specific Labeling Procedure[a]

	k_a ($\times 10^5$ M^{-1} s^{-1})	k_d ($\times 10^{-4}$ s^{-1})	K_D ($\times 10^{-9}$ M)
2Rs15d-H	2.4 ± 0.0	7.5 ± 0.1	**3.1 ± 0.0**
CHX-A″-DTPA-2Rs15d-H	1.3 ± 0.0	6.6 ± 0.1	**5.1 ± 0.1**
2Rs15d-HLC (after fresh reduction)	1.4 ± 0.0	7.5 ± 0.1	**5.3 ± 0.1**
DTPA-2Rs15d-HLC	1.3 ± 0.0	7.6 ± 0.1	**5.9 ± 0.1**
In-DTPA-2Rs15d-HLC	1.0 ± 0.0	5.9 ± 0.0	**6.2 ± 0.0**

[a]The kinetic parameters (association reaction rate constant k_a, dissociation reaction rate constant k_d, and dissociation equilibrium constant K_D; ±SE) were determined via surface plasmon resonance on immobilized HER2 recombinant protein. The kinetic parameters of unconjugated sdAb 2Rs15d-H and the lysine-conjugated sdAb CHX-A″-DTPA-2Rs15d-H are given as a reference. In-DTPA-2Rs15d-HLC was measured after cold labeling of the probe.

excess of cold sdAb 2Rs15d-H (Figure 3). Moreover, binding was significantly higher compared to the nontargeting control sdAb ^{111}In-DTPA-BcII10-HLC. A similar cell binding capacity was obtained when sdAb 2Rs15d was either site-specifically labeled on the cysteine or randomly labeled on the lysines.

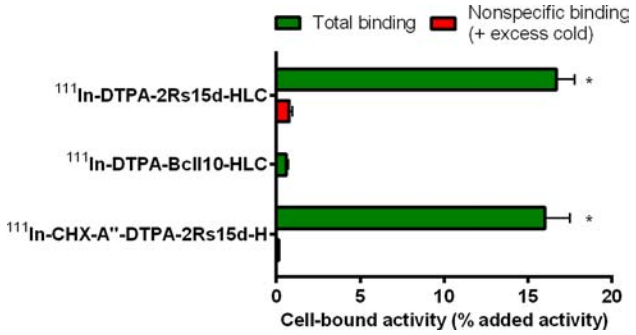

Figure 3. ^{111}In-DTPA-2Rs15d-HLC retained its binding specificity for HER2-positive SKOV3 cells. Binding specificity was assessed by the determination of total binding and nonspecific binding, the latter by coincubation with a 1000-fold molar excess of unlabeled 2Rs15d-H. Binding of ^{111}In-DTPA-2Rs15d-HLC and ^{111}In-CHX-A″-DTPA-2Rs15d-H was significantly different from the control sdAb ^{111}In-DTPA-BcII10-HLC (* $p < 0.05$).

***In Vivo* Characterization.** As a final step in the validation of the site-specific labeling strategy, we investigated whether the tracers were still able to target HER2-positive tumors *in vivo*. The site-specifically labeled sdAb ^{111}In-DTPA-2Rs15d-HLC, the randomly labeled sdAb ^{111}In-CHX-A″-DTPA-2Rs15d-H, and the site-specifically labeled nontargeting control sdAb ^{111}In-DTPA-BcII10-HLC were administered to three groups of SKOV3-xenografted nude mice, bearing a subcutaneous HER2-positive tumor. SPECT-Computed Tomography (CT) imaging was performed 1 h after administration of the sdAb. These images demonstrate that the site-specifically labeled tracer ^{111}In-DTPA-2Rs15d-HLC was still functional *in vivo* and was able to visualize the tumor already 1 h postinjection, in contrast to the nontargeting control sdAb ^{111}In-DTPA-BcII10-HLC (Figure 4). Besides the tumor, the kidneys and urinary bladder were also visible (Figure S3, Supporting Information), which corresponded to the typical renal excretion pattern of sdAbs and other small sized probes. Abdominal activity was furthermore observed in all three groups of animals, presumably due to some extent of hepatobiliary clearance.

The targeting capacities were confirmed by *ex vivo* quantification after euthanasia and dissection at 90 min postinjection (Table 3). Tumor uptake of the site-specifically labeled sdAb ^{111}In-DTPA-2Rs15d-HLC (4.43% ± 1.50% injected activity per gram (% IA/g)) was significantly higher ($p < 0.05$) than with nontargeting control sdAb ^{111}In-DTPA-BcII10-HLC (0.41% ± 0.09% IA/g). Uptake was low in all other nontarget organs (<0.50% IA/g), except for kidneys. Similar results were obtained for the randomly labeled sdAb ^{111}In-CHX-A″-DTPA-2Rs15d-H, whereby low background and high tumor contrast values at an early time point were also obtained. These data demonstrated that the site-specifically labeled sdAb retained its functionality as an imaging tracer after reduction with 2-MEA, site-specific conjugation with a maleimide-functionalized chelating agent, and radiolabeling.

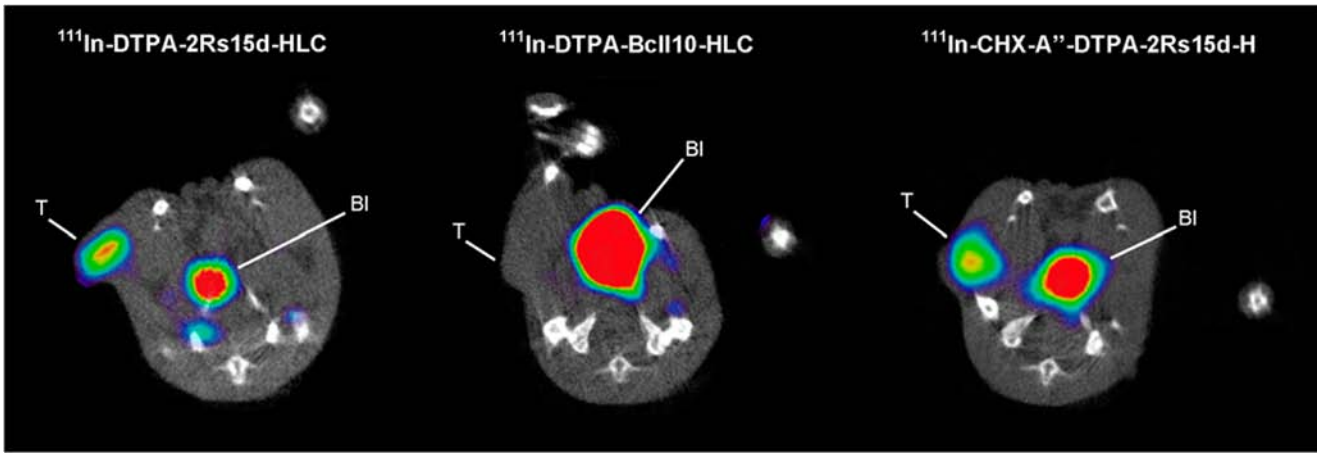

Figure 4. Site-specifically labeled sdAb ^{111}In-DTPA-2Rs15d-HLC proved to be functional *in vivo*. It was able to visualize the tumor (T) in SPECT-CT imaging of HER2-positive SKOV3 xenografts already at 1 h postinjection (transverse sections are shown). The urinary bladder (Bl) was also seen due to the renal excretion of sdAbs. Similar images were obtained for the lysine-conjugated ^{111}In-CHX-A″-DTPA-2Rs15d-H, while the nontargeting control sdAb ^{111}In-DTPA-BcII10-HLC was not accumulating in the tumor.

dx.doi.org/10.1021/bc500111t | *Bioconjugate Chem.* 2014, 25, 979−988

Table 3. Site-Specifically Labeled sdAb ^{111}In-DTPA-2Rs15d-HLC Accumulates Significantly in the Tumor with Low Background Values (Except Kidneys)[a]

	site-specific ^{111}In-DTPA-2Rs15d-HLC	site-specific ^{111}In-DTPA-BcII10-HLC	random (lysine) ^{111}In-CHX-A″-DTPA 2Rs15d-H
blood	0.44 ± 0.06	0.42 ± 0.07	0.31 ± 0.11
heart	0.15 ± 0.03	0.14 ± 0.04	0.32 ± 0.05[c]
lungs	0.40 ± 0.10	0.62 ± 0.13	0.64 ± 0.33
liver	0.41 ± 0.04[b]	0.32 ± 0.03	1.67 ± 0.39[c]
spleen	0.20 ± 0.04	0.19 ± 0.03	0.40 ± 0.09[c]
small intestine	0.16 ± 0.09	0.24 ± 0.17	0.25 ± 0.15
kidney	267.14 ± 19.94	288.80 ± 41.44	294.70 ± 15.90
muscle	0.17 ± 0.09	0.19 ± 0.04	0.27 ± 0.09
tumor	4.43 ± 1.50[b]	0.41 ± 0.09	5.95 ± 1.11[b]
tumor/blood	10.03 ± 3.18[b]	0.97 ± 0.11	21.38 ± 9.56[b]
tumor/muscle	27.97 ± 7.48[b]	2.12 ± 0.35	23.03 ± 5.86[b]

[a]Biodistribution profile of ^{111}In-labeled sdAbs in HER2-positive SKOV3 xenografts at 90 min postinjection was determined *ex vivo*. Values are expressed as % IA/g ± SD. [b]Significantly different from control sdAb ^{111}In-DTPA-BcII10-HLC ($p < 0.05$). [c]Significantly different from both site-specifically labeled sdAbs ($p < 0.05$).

DISCUSSION

Site-specific labeling of probes for molecular imaging is of great interest to obtain homogeneous tracer populations with a well-defined stoichiometry and label position, preventing antigen binding interference after conjugation and allowing a batch-to-batch reproducible characterization for clinical translation. Currently the site-specific labeling of sdAbs is already possible via ^{99m}Tc complexation of the carboxyl-terminal hexahistidine tag with tricarbonyl chemistry.[25] However, this type of labeling is only available for preclinical use, since the hexahistidine tag is omitted in clinical translation.[14] Therefore, an alternative labeling strategy via a thio-ether bond was investigated. This strategy allows the development of a generic method that enables the extension of ^{99m}Tc SPECT imaging to a multimodal level with SPECT (^{111}In), positron emission tomography (^{18}F, ^{68}Ga, ^{64}Cu), optical imaging (near-infrared), and radionuclide therapy (^{177}Lu, ^{125}I, ^{131}I).

The introduction of an unpaired cysteine for site-specific conjugation to sdAbs has already been described earlier.[26−30] However, the precise format of the cysteine-construct, its corresponding influence on the production yield, and the necessity of a reduction step due to the presence of dimeric sdAbs and blocked monomeric sdAbs were frequently not reported. Moreover, the homogeneity of these probes was never analyzed via mass spectrometry. Here we present a full description of the production and conjugation process of a sdAb with an engineered unpaired cysteine, for its use in molecular imaging.

The introduction of an unpaired cysteine showed a sdAb sequence-independent and cysteine position-dependent negative effect on the production yield. Probably, an inappropriately positioned unpaired cysteine leads to folding problems in the bacterial expression system and to bacteria toxification as illustrated by less turbid cultures after overnight expression and viscous periplasmic extracts. The influence of cysteine residues on the production yield of sdAbs has been described before: the introduction of an additional (third) disulfide bond showed a 5-fold reduction in production yields,[31] while elimination of the interloop disulfide bond could lead to a 20-fold increase in the production yield of the sdAb.[32] It is likely that the introduction of an unpaired cysteine disturbs correct sdAb folding even further. scFv's and diabodies also show reduced production yields after addition of a carboxyl-terminal cysteine, while elimination of an unpaired cysteine improves yield and purity after affinity chromatography.[33] The introduction of an unpaired cysteine positioned further away from the sdAb sequence in the sdAb-HLC construct did, however, show a less dramatic effect on the production yields, probably due to a less severe influence on sdAb folding.

After expression and purification of the sdAb-HLC construct, the presence of blocked monomeric sdAb was detected after ESI-Q-ToF mass spectrometry analysis. The observed mass increase of 306 Da probably corresponds to a glutathione molecule, of which the expected mass in its reduced state is 307 Da, bound to the unpaired cysteine of monomeric sdAb. It has already been observed that unpaired cysteines introduced in antibodies are capped with glutathione or cysteine upon mammalian cell expression.[8,34] It is highly plausible that this also happens in a bacterial expression system, since there are indications that glutathione is also present in the *Escherichia coli* periplasm.[35]

From the mixture obtained after expression and purification of sdAb-HLC, only the fraction monomeric sdAbs with uncapped cysteine is directly available for site-specific conjugation. A reduction reaction was thus introduced to reduce the dimeric and blocked monomeric sdAbs. Although both TCEP[26,30] and DTT[29] have already been used with sdAbs, we preferred to use the mild reducing agent 2-MEA to prevent reduction of the conserved internal disulfide bond, which is crucial for stability of antibody domains. The reduction reaction of sdAb-HLC (at a final concentration of 1 mg/mL) was optimized to be performed with a 180-fold molar excess of 2-MEA and incubation for 90 min at 37 °C, in order to reduce all dimers, retain antigen-binding capacity, and prevent reduction of the interloop disulfide bond (present in sdAb 2Rs15d). To maintain the unpaired cysteine in its reduced form the buffers used during reduction and conjugation were aerated with N_2 and supplemented with 5 mM EDTA. Besides in monomeric sdAb, the reduction reaction also resulted in the formation of monomeric sdAb bound to 2-MEA. 2-MEA follows, similar to DTT, a two-step reduction process with the formation of a mixed disulfide (sdAb-2-MEA) as a reaction intermediate.[36]

After reduction, the buffer was changed to 0.2 M NH_4OAc (pH 6.5) to lower the pH of the subsequent maleimide conjugation reaction and avoid the formation of deprotonated amines that might react with maleimide. This pH-controlled reaction led to the formation of a homogeneous tracer population with single conjugated sdAbs.

The functionality of the site-specifically labeled sdAb was validated in the HER2 cancer model. After reduction with 2-MEA, conjugation to maleimide-DTPA, and radiolabeling with ^{111}In, sdAb 2Rs15d-HLC was still able to bind recombinant HER2 protein with similar affinity, bind HER2-expressing cells specifically, and image HER2-positive tumors with high contrast at early time points after injection. Besides the significant tumor uptake in SKOV3 xenografted mice, the typical renal excretion pattern of sdAbs was also observed.[37] The activity uptake in the kidneys is in this case even augmented by the use of the residualizing radiometal ^{111}In.

dx.doi.org/10.1021/bc500111t | *Bioconjugate Chem.* 2014, 25, 979−988

Similar *in vitro* and *in vivo* HER2-targeting capacities were obtained for the site-specifically and the randomly labeled sdAb 2Rs15d. Conversely, Kijanka et al.[30] encountered loss of sdAb binding affinity upon conjugation to the primary amines of lysine residues. They attributed this to the presence of lysine residues present in or near the antigen-binding region. This illustrates the high sequence dependency of conjugation strategies to lysine residues, which can be avoided by the introduction of an unpaired cysteine for site-specific conjugation. The comparable results obtained for site-specifically and randomly labeled 2Rs15d should come as no surprise since one of the selection criteria for 2Rs15d as a lead compound was the absence of a lysine in its antigen-binding region.[13] Therefore, this study confirms furthermore that labeling the lysine residues in our clinical lead compound 2Rs15d[14] does not impede its functionality.

Of note, the comparison between the site-specifically and the randomly labeled sdAb 2Rs15d could be influenced possibly by the use of two analogues of the chelating agent, DTPA and CHX-A″-DTPA, respectively. CHX-A″-DTPA is known to complex indium with a higher kinetic inertness than DTPA.[38] Nevertheless, the radiolabeled complex ^{111}In-DTPA-sdAb-HLC was shown to be stable *in vitro* in PBS (97% intact complex after 3 h) and human blood plasma (97% intact complex after 90 min, 93% after 24 h) which makes it plausible that there is no decomposition of the complex at the early time point of sdAb imaging (1 h postinjection). The similar biodistribution profiles obtained with ^{111}In-DTPA-2Rs15d-HLC and ^{111}In-CHX-A″-DTPA-2Rs15d-H at 90 min postinjection (with no significant difference in blood levels and tumor uptake) supports the assumption that both chelating agents provide comparable results at early time points. Moreover, similar results between both DTPA variants in *in vitro* and *in vivo* experiments with small-sized imaging probes already have been observed previously as well.[39]

In conclusion, we presented a generic strategy for site-specific labeling of sdAbs and demonstrated that the site-specifically labeled sdAb retained its functionality as an imaging tracer after reduction with 2-MEA, site-specific conjugation with a maleimide-functionalized chelating agent, and radiolabeling. The final product was shown to be homogeneous, which is important for future clinical translation.

EXPERIMENTAL PROCEDURES

sdAb Engineering, Production, and Purification. The generation and biochemical characterization of anti-HER2 sdAb 2Rs15d and control sdAb BcII10 have been described previously.[13,40] sdAb-H, sdAb-HC, and sdAb-HLC constructs (Scheme 1A) were made by ligating the sdAb coding regions in-frame in, respectively, the pHEN6, pHEN26, and pHEN25 plasmids. The pHEN6 plasmid has been described before.[40] It is an *E. coli* expression plasmid containing the coding region for the seven first and eight last conserved sdAb amino acids that are followed by a hexahistidine tag and flanked with unique restriction enzyme recognition sites. Plasmids pHEN25 and pHEN26 are derivatives from pHEN6. pHEN26 encodes for an additional cysteine after the hexahistidine tag. It was created according to the 'ligation during amplification' method with phosphorylated primers M13R (GGATAACAATTTCACAC-AGG) and His6C-AS (TGAATTCTATTAACAGTGAT-GGTGATG) on the pHen6 plasmid.[41] In pHEN25, the sdAb amino-terminal glutamine was mutated into glutamic acid and a 14-amino-acid-long linker and cysteine (SPSTPPTPSPSTPPC) were introduced after the hexahistidine tag. This derivative was obtained by amplification of the multiple cloning site of the pHen6 plasmid with PCR primers UZO-FP (CGGCCATG-GCCGAGGTGCAGCTG) and UZO-*RP* (AGTGAATTC-TATTAACACGGTGGTGTGGATGGTGATGGTGTGGGA-GGTGTAGATGGGCTGTGATGGTGATGGTGGTGTGA-GG) and ligating it into a pHen6 plasmid, after NcoI and *Eco*RI digestion.

All sdAbs (with and without unpaired cysteine) were produced in *E. coli* WK6 cells and purified via periplasmic extraction, immobilized metal affinity chromatography and SEC, as described in detail elsewhere.[42] In short, sdAbs were secreted to the periplasm of the bacterial host, from which they were collected via an osmotic shock. sdAbs were purified from the periplasmic extract via immobilized metal affinity chromatography with HIS-select solution (Sigma-Aldrich) and subsequent SEC on a HiLoad 16/600 Superdex 75 PG column (GE Healthcare) with elution in PBS (pH 7.4).

sdAb concentrations were determined spectrophotometrically at 280 nm with the theoretically calculated extinction coefficient.[43]

ESI-Q-ToF Mass Spectrometry. Desalting and buffer exchange to 25 mM NH_4OAc of samples was done using Amicon (MWCO 3000) (Millipore) according to manufacturer's protocol. The samples were analyzed by ESI-Q-ToF (Waters, Micromass) in positive ion mode at an estimated sdAb concentration of 10 μM in 25 mM NH_4OAc with 30% acetonitrile and 0.5% formic acid. Spectrum deconvolutions were calculated using the maximum entropy with Max ent1. Theoretical masses were calculated using ChemBioDraw Ultra 13.0 (PerkinElmer).

Buffers. All buffers used for reduction, conjugation, and radiolabeling were purified from metal contamination using Chelex-100 (Sigma-Alrich), passed through a 0.22 μm filter, and aerated with N_2 before use.

Reduction with 2-MEA and Conjugation to a Bifunctional Ligand. sdAb-HLC (2 to 3 mg, 1 mg/mL final concentration) was reduced by addition of 180-fold molar excess of 2-MEA hydrochloride (Acros Organics) in PBS (pH 7.4) with 5 mM EDTA. After incubation for 90 min at 37 °C, the reduced sdAb solution was buffer exchanged to 0.2 M NH_4OAc (pH 6.0−6.5) with 5 mM EDTA using PD-10 desalting columns (GE Healthcare) according to manufacturer's protocol. For site-specific conjugation a 10-fold molar excess of maleimide-DTPA (2,2′-(1-carboxy-2-(carboxymethyl)-13-(2,5-dioxo-2,5-dihydro-1*H*-pyrrol-1-yl)-10-oxo-2,5,8,11-tetraazatridecane-5,8-diyl)diacetic acid; $C_{20}H_{29}N_5O_{11}$·TFA; Chematech) was added to the reduced sdAb and incubated for 2 h at 37 °C. The conjugated sdAb solution was concentrated with Vivaspin 2 (MWCO 5000) (Sartorius) according to manufacturer's protocol, prior to purification from excess maleimide-DTPA and reduction intermediate via SEC on a Superdex 75 10/300 GL column (GE Healthcare) with elution in 0.1 M NH_4OAc (pH 7.0). The concentration of the conjugate was determined similarly to unconjugated sdAb, assuming that maleimide-DTPA did not significantly change the extinction coefficient at 280 nm.

sdAbs without an introduced unpaired cysteine (sdAb-H) were randomly conjugated to CHX-A″-DTPA (*N*-[(*R*)-2-Amino-3-(4-isothiocyanatophenyl)propyl]-trans-(*S*,*S*)-cyclohexane-1,2-diamine-*N*,*N*′,*N*″,*N*″-pentaacetic acid; $C_{26}H_{34}N_4O_{10}S$·3HCl; Macrocyclics) on their lysine residues

dx.doi.org/10.1021/bc500111t | *Bioconjugate Chem.* 2014, 25, 979−988

as previously described.[44] A heterogeneous mixture was obtained of sdAbs derivatized with 0, 1, and 2 chelating agents.

Radiolabeling with ^{111}In and Determination of Radiochemical Purity. DTPA-conjugated sdAbs (1 to 5 nmol, 10^{-5} M final concentration) were radiolabeled with $^{111}InCl_3$ (Mallinckrodt Pharmaceuticals) (14.8 to 177.6 MBq) in 0.2 M NH_4OAc (pH 5.0) by incubation for 30 min at room temperature, 37 or 50 °C. Radiochemical purity was analyzed by iTLC on silica gel (Pall Corporation) using 0.1 M sodium citrate (pH 5.0) as the eluent. The radiolabeled tracer was further purified via gel-filtration chromatography with a PBS-Tween (0.1%) pre-equilibrated NAP-5 column (GE Healthcare) according to manufacturer's protocol. Prior to *in vivo* use, the radiolabeled tracers were passed through a 0.22 μm filter.

RP-HPLC. RP-HPLC analysis of radiotracer was performed on a polystyrene divinylbenzene copolymer column (PLRP-S 300 Å, 5 μm, 250/4 mm; Varian) with the following gradient (A: 0.1% trifluoroacetic acid in water; B: 0.1% trifuoroacetic acid in acetonitrile): 0−5 min, 25% B; 5−7 min, 25%−34% B; 7−10 min, 75%−100% B; 10−20 min, 100% B; at a flow rate of 1 mL/min.

Stability in Human Blood Plasma. The plasma stability was determined by incubating ^{111}In-DTPA-sdAb-HLC (0.5 nmol in 200 μL) with 400 μL human blood plasma at 37 °C. At specific time points the mixture was analyzed by SEC on a Superdex 75 10/300 GL column (GE Healthcare) with elution in PBS at a speed of 0.5 mL/min.

Cold Labeling with Indium. sdAbs were cold labeled with indium for surface plasmon resonance measurements. The site-specific conjugated sdAb DTPA-2Rs15d-HLC was incubated with a 5-fold molar excess of $InCl_3$ (Sigma-Aldrich) in 0.1 M NH_4OAc (pH 5.0) for 2 h at room temperature. The cold labeled sdAb was purified from excess $InCl_3$ via SEC on a Superdex 75 10/300 GL column (GE Healthcare) with elution in 0.1 M NH_4OAc (pH 7.0).

Surface Plasmon Resonance. Affinity measurements were performed on a Biacore T200 (GE Healthcare). Recombinant HER2-Fc protein (Sino Biologicals) in sodium acetate (pH 4.5) was immobilized on a CM5 chip to 740 response units (RU). Analyte flow was 10 μL/min in HBS and the chip was regenerated using 100 mM glycine-HCl (pH 2.0). sdAbs were analyzed in a 2-fold serial dilution (125−0.488 nM). The association phase took 180 s and the dissociation phase 600 s. Binding curves were fitted using a '1:1 (antigen:analyte) with drift and RI2' binding model in Biacore T200 evaluation software.

Cells and Culturing Conditions. The human HER2-positive ovarian cancer cell line SKOV3 was obtained from American Type Culture Collection and cultured as previously described.[13]

***In Vitro* Cell Binding Study.** 10^5 SKOV3 cells were adhered overnight in a 24-well plate (Greiner). ^{111}In-labeled sdAbs were incubated at a final concentration of 10 nM in DMEM medium (500 μL total volume). Nonspecific binding was assessed by including a 1000-fold excess of the unlabeled sdAb-H construct. After 1 h incubation at 37 °C, cells were washed three times with ice-cold PBS-Tween (0.1%) and subsequently detached by incubation for 30 min at room temperature in 1 mL NaOH. After cell collection the bound activity was counted in a gamma counter (Cobra II inspector 5003, Canberra-Packard) and expressed as percentage of added activity. The latter was determined by measuring the same amount of added radiolabeled tracer in PBS (1 mL total volume). All measurements were performed in triplicate.

Animal Model. All animal study protocols were approved by the Ethical committee for animal experiments of Vrije Universiteit Brussel. Female athymic nude mice (Harlan) were subcutaneously injected with 10^7 SKOV3 cells in PBS (pH 7.4) in the right hind leg, under the control of 2.5% isoflurane (Abbott). Tumors were grown for 15 days (34 to 129 mg).

SPECT-CT Imaging and *ex Vivo* Biodistribution Analysis. SKOV3 xenografts (n = 4−6) were intravenously injected under the control of 2.5% isoflurane (Abbott) with either ^{111}In-DTPA-2Rs15d-HLC, ^{111}In-CHX-A″-DTPA-2Rs15d-H, or ^{111}In-DTPA-BcII10-HLC for *ex vivo* biodistribution analysis (3 μg−2.4 MBq−13 MBq/nmol). In each group of six mice, three received a higher dose of radiolabeled tracer (5 μg−4.4 MBq−13 MBq/nmol) for additional SPECT-CT imaging.

Prior to SPECT-CT acquisition mice were anesthetized by intraperitoneal injection with a mixture of 18.75 mg/kg ketamine hydrochloride (Ketamine 1000, CEVA) and 0.5 mg/kg medetomidine hydrochloride (Domitor, Pfizer). At 1 h postinjection micro-CT imaging was followed by pinhole SPECT on separate systems. Image acquisition and reconstruction were performed as described previously.[45] In brief, micro-CT was performed using a dual-source CT scanner (Skyscan 1178, Skyscan) with 60 kV and 615 mA at a resolution of 83 μm. The scan time was 2 min. Images were reconstructed using filtered backprojection (NRecon, Skyscan). Pinhole SPECT was performed using a dual-headed gamma camera (e.cam180, Siemens), equipped with 2 single pinhole collimators (1.5 mm pinhole opening, 250 mm focal length, 47 mm radius of rotation). Images were acquired over 360° in 64 projections of 20 s into a 128 × 128 matrix. The SPECT images were reconstructed using an iterative reconstruction algorithm adapted for single pinhole (based on the ordered-subset expectation maximization scheme) and automatically reoriented for fusion with CT images based on six ^{57}Co sources. Images were analyzed using OsiriX (Pixmeo).

Animals were dissected at 90 min postinjection and organ activities were measured against a standard of known activity with a gamma counter (Cobra II inspector 5003, Canberra-Packard) and expressed as percentage of injected activity per gram of tissue, corrected for decay.

Statistical Analysis. The statistical analysis was performed in SPSS Statistics 22 (IBM). Data sets were analyzed using a one-way ANOVA with Tukey post hoc correction for equal assumed variances and Games-Howell correction for unequal assumed variances, based on Levene's test.

■ ASSOCIATED CONTENT

Ⓢ Supporting Information

Supplementary experimental procedures; characterization of the purified sdAb-HLC after production; and whole-body SPECT-CT imaging of HER2-positive SKOV3 xenografts at 1 h postinjection are presented. This material is available free of charge via the Internet at http://pubs.acs.org.

■ AUTHOR INFORMATION

Corresponding Author

*E-mail address: ndevoogd@vub.ac.be. Phone: +32 (0)2 629 19 78. Fax: +32 (0)2 629 19 81.

Notes

The authors declare no competing financial interest.

■ ACKNOWLEDGMENTS

The authors thank Cindy Peleman for technical assistance with the imaging experiments. Sam Massa and Jens De Vos are PhD fellows of the Research Foundation − Flanders (FWO). Tony Lahoutte is a Senior Clinical Investigator of the Research Foundation − Flanders (FWO). The research at ICMI laboratory is funded by the Belgian State, Nationaal Kankerplan, Vlaamse Liga tegen Kanker, Stichting tegen Kanker, FWO, IWT, and Vrije Universiteit Brussel.

■ ABBREVIATIONS

sdAb, camelid single-domain antibody-fragment; HER2, human epidermal growth factor receptor 2; SPECT, single-photon emission computed tomography; SEC, size-exclusion chromatography; LDS-PAGE, lithiumdodecylsulfate polyacrylamide gel electrophoresis; ESI-Q-ToF, electrospray ionization quadrupole time-of-flight; 2-MEA, 2-mercaptoethylamine; iTLC, instant thin-layer chromatography; RP-HPLC, reverse-phase HPLC; CT, computed tomography; % IA/g, % injected activity per gram

■ REFERENCES

(1) Wang, L. T., Amphlett, G., Blattler, W. A., Lambert, J. M., and Zhang, W. (2005) Structural characterization of the maytansinoid - monoclonal antibody immunoconjugate, huN901-DM1, by mass spectrometry. *Protein Sci. 14*, 2436−2446.

(2) Sun, M. M. C., Beam, K. S., Cerveny, C. G., Hamblett, K. J., Blackmore, R. S., Torgov, M. Y., Handley, F. G. M., Ihle, N. C., Senter, P. D., and Alley, S. C. (2005) Reduction-alkylation strategies for the modification of specific monoclonal antibody disulfides. *Bioconjugate Chem. 16*, 1282−1290.

(3) Hamblett, K. J., Senter, P. D., Chace, D. F., Sun, M. M. C., Lenox, J., Cerveny, C. G., Kissler, K. M., Bernhardt, S. X., Kopcha, A. K., Zabinski, R. F., Meyer, D. L., and Francisco, J. A. (2004) Effects of drug loading on the antitumor activity of a monoclonal antibody drug conjugate. *Clin. Cancer Res. 10*, 7063−7070.

(4) Shin, I. S., Lee, S. M., Kim, H. S., Yao, Z. S., Regino, C., Sato, N., Cheng, K. T., Hassan, R., Campo, M. F., Albone, E. F., Choyke, P. L., Pastan, I., and Paik, C. H. (2011) Effect of chelator conjugation level and injection dose on tumor and organ uptake of In-111-labeled MORAb-009, an anti-mesothelin antibody. *Nucl. Med. Biol. 38*, 1119−1127.

(5) Shen, B.-Q., Xu, K., Liu, L., Raab, H., Bhakta, S., Kenrick, M., Parsons-Reponte, K. L., Tien, J., Yu, S.-F., Mai, E., Li, D., Tibbitts, J., Baudys, J., Saad, O. M., Scales, S. J., McDonald, P. J., Hass, P. E., Eigenbrot, C., Nguyen, T., Solis, W. A., Fuji, R. N., Flagella, K. M., Patel, D., Spencer, S. D., Khawli, L. A., Ebens, A., Wong, W. L., Vandlen, R., Kaur, S., Sliwkowski, M. X., Scheller, R. H., Polakis, P., and Junutula, J. R. (2012) Conjugation site modulates the in vivo stability and therapeutic activity of antibody-drug conjugates. *Nat. Biotechnol. 30*, 184−189.

(6) Albrecht, H., Burke, P. A., Natarajan, A., Xiong, C. Y., Kalicinsky, M., DeNardo, G. L., and DeNardo, S. J. (2004) Production of soluble ScFvs with C-terminal-free thiol for site-specific conjugation or stable dimeric ScFvs on demand. *Bioconjugate Chem. 15*, 16−26.

(7) Olafsen, T., Cheung, C. W., Yazaki, P. J., Li, L., Sundaresan, G., Gambhir, S. S., Sherman, M. A., Williams, L. E., Shively, J. E., Raubitschek, A. A., and Wul, A. M. (2004) Covalent disulfide-linked anti-CEA diabody allows site-specific conjugation and radiolabeling for tumor targeting applications. *Protein Eng., Des., Sel. 17*, 21−27.

(8) Junutula, J. R., Raab, H., Clark, S., Bhakta, S., Leipold, D. D., Weir, S., Chen, Y., Simpson, M., Tsai, S. P., Dennis, M. S., Lu, Y. M., Meng, Y. G., Ng, C., Yang, J. H., Lee, C. C., Duenas, E., Gorrell, J., Katta, V., Kim, A., McDorman, K., Flagella, K., Venook, R., Ross, S., Spencer, S. D., Wong, W. L., Lowman, H. B., Vandlen, R., Sliwkowski, M. X., Scheller, R. H., Polakis, P., and Mallet, W. (2008) Site-specific conjugation of a cytotoxic drug to an antibody improves the therapeutic index. *Nat. Biotechnol. 26*, 925−932.

(9) Hamers-Casterman, C., Atarhouch, T., Muyldermans, S., Robinson, G., Hamers, C., Songa, E. B., Bendahman, N., and Hamers, R. (1993) Naturally-occuring antibodies devoid of light-chains. *Nature 363*, 446−448.

(10) Muyldermans, S. (2013) Nanobodies: natural single-domain antibodies. *Annu. Rev. Biochem. 82*, 775−797.

(11) Vaneycken, I., D'huyvetter, M., Hernot, S., De Vos, J., Xavier, C., Devoogdt, N., Caveliers, V., and Lahoutte, T. (2011) Immuno-imaging using nanobodies. *Curr. Opin. Biotechnol. 22*, 877−881.

(12) De Vos, J., Devoogdt, N., Lahoutte, T., and Muyldermans, S. (2013) Camelid single-domain antibody-fragment engineering for (pre)clinical in vivo molecular imaging applications: adjusting the bullet to its target. *Expert Opin. Biol. Ther. 13*, 1149−1160.

(13) Vaneycken, I., Devoogdt, N., Van Gassen, N., Vincke, C., Xavier, C., Wernery, U., Muyldermans, S., Lahoutte, T., and Caveliers, V. (2011) Preclinical screening of anti-HER2 nanobodies for molecular imaging of breast cancer. *FASEB J. 25*, 2433−2446.

(14) Xavier, C., Vaneycken, I., D'Huyvetter, M., Heemskerk, J., Keyaerts, M., Vincke, C., Devoogdt, N., Muyldermans, S., Lahoutte, T., and Caveliers, V. (2013) Synthesis, Preclinical validation, dosimetry, and toxicity of Ga-68-NOTA-Anti-HER2 nanobodies for iPET imaging of HER2 receptor expression in cancer. *J. Nucl. Med. 54*, 776−784.

(15) Vaneycken, I., Govaert, J., Vincke, C., Caveliers, V., Lahoutte, T., De Baetselier, P., Raes, G., Bossuyt, A., Muyldermans, S., and Devoogdt, N. (2010) In vitro analysis and in vivo tumor targeting of a humanized, grafted nanobody in mice using pinhole SPECT/Micro-CT. *J. Nucl. Med. 51*, 1099−1106.

(16) Gainkam, L. O. T., Huang, L., Caveliers, V., Keyaerts, M., Hernot, S., Vaneycken, I., Vanhove, C., Revets, H., De Baetselier, P., and Lahoutte, T. (2008) Comparison of the biodistribution and tumor targeting of two Tc-99m-labeled anti-EGFR nanobodies in mice, using pinhole SPECT/micro-CT. *J. Nucl. Med. 49*, 788−795.

(17) Lemaire, M., D'Huyvetter, M., Lahoutte, T., Van Valckenborgh, E., Menu, E., De Bruyne, E., Kronenberger, P., Wernery, U., Muyldermans, S., Devoogdt, N., and Vanderkerken, K. (2014) Imaging and radioimmunotherapy of multiple myeloma with anti-idiotypic nanobodies. *Leukemia 28*, 444−447.

(18) Broisat, A., Hernot, S., Toczek, J., De Vos, J., Riou, L. M., Martin, S., Ahmadi, M., Caveliers, V., Muyldermans, S., Lahoutte, T., Fagret, D., Ghezzi, C., and Devoogdt, N. (2012) Anti mouse/human VCAM1 nanobodies for SPECT imaging of atherosclerosis. *J. Nucl. Med. 53*, 665−666.

(19) De Vos, J., Mathijs, I., Xavier, C., Massa, S., Wernery, U., Bouwens, L., Lahoutte, T., Muyldermans, S., and Devoogdt, N. Specific targeting of atherosclerotic plaques in ApoE−/− mice using a new camelid sdAb binding the vulnerable plaque marker LOX-1. *Molecular Imaging and Biology*, [Online early access]. DOI: 10.1007/s11307-014-0731-6. Published Online: Apr 1, 2014.

(20) Movahedi, K., Schoonooghe, S., Laoui, D., Houbracken, I., Waelput, W., Breckpot, K., Bouwens, L., Lahoutte, T., De Baetselier, P., Raes, G., Devoogdt, N., and Van Ginderachter, J. A. (2012) Nanobody-based targeting of the macrophage mannose receptor for effective in vivo imaging of tumor-associated macrophages. *Cancer Res. 72*, 4165−4177.

(21) Put, S., Schoonooghe, S., Devoogdt, N., Schurgers, E., Avau, A., Mitera, T., D'Huyvetter, M., De Baetselier, P., Raes, G., Lahoutte, T., and Matthys, P. (2013) SPECT imaging of joint inflammation with nanobodies targeting the macrophage mannose receptor in a mouse model for rheumatoid arthritis. *J. Nucl. Med. 54*, 807−814.

(22) Zheng, F., Put, S., Bouwens, L., Lahoutte, T., Matthys, P., Muyldermans, S., De Baetselier, P., Devoogdt, N., Raes, G., and Schoonooghe, S. Molecular imaging with macrophage CRIg-targeting nanobodies for early and preclinical diagnosis in a mouse model of

rheumatoid arthritis. *J. Nucl. Med.*, [Online early access]. DOI: 10.2967/jnumed.113.130617. Published online: Mar 31, 2014.
(23) Vincke, C., Loris, R., Saerens, D., Martinez-Rodriguez, S., Muyldermans, S., and Conrath, K. (2009) General strategy to humanize a camelid single-domain antibody and identification of a universal humanized nanobody scaffold. *J. Biol. Chem. 284*, 3273−3284.
(24) Lambert, C., Leonard, N., De Bolle, X., and Depiereux, E. (2002) ESyPred3D: Prediction of proteins 3D structures. *Bioinformatics 18*, 1250−1256.
(25) Xavier, C., Devoogdt, N., Hernot, S., Vaneycken, I., D'Huyvetter, M., De Vos, J., Massa, S., Lahoutte, T., and Caveliers, V. (2012) Site-specific labeling of his-tagged Nanobodies with 99mTc: a practical guide. *Methods Mol. Biol. 911*, 485−90.
(26) Sadeqzadeh, E., Rahbarizadeh, F., Ahmadvand, D., Rasaee, M. J., Parhamifar, L., and Moghimi, S. M. (2011) Combined MUC1-specific nanobody-tagged PEG-polyethylenimine polyplex targeting and transcriptional targeting of tBid transgene for directed killing of MUC1 over-expressing tumour cells. *J. Controlled Release 156*, 85−91.
(27) Sukhanova, A., Even-Desrumeaux, K., Kisserli, A., Tabary, T., Reveil, B., Millot, J.-M., Chames, P., Baty, D., Artemyev, M., Oleinikov, V., Pluot, M., Cohen, J. H. M., and Nabiev, I. (2012) Oriented conjugates of single-domain antibodies and quantum dots: toward a new generation of ultrasmall diagnostic nanoprobes. *Nanomedicine (N. Y., NY, U. S.) 8*, 516−525.
(28) Van de Broek, B., Devoogdt, N., D'Hollander, A., Gijs, H.-L., Jans, K., Lagae, L., Muyldermans, S., Maes, G., and Borghs, G. (2011) Specific cell targeting with nanobody conjugated branched gold nanoparticles for photothermal therapy. *ACS Nano 5*, 4319−4328.
(29) Vugmeyster, Y., Entrican, C. A., Joyce, A. P., Lawrence-Henderson, R. F., Leary, B. A., Mahoney, C. S., Patel, H. K., Raso, S. W., Olland, S. H., Hegen, M., and Xu, X. (2012) Pharmacokinetic, biodistribution, and biophysical profiles of TNF nanobodies conjugated to linear or branched poly(ethylene glycol). *Bioconjugate Chem. 23*, 1452−1462.
(30) Kijanka, M., Warnders, F. J., El Khattabi, M., Lub-de Hooge, M., van Dam, G. M., Ntziachristos, V., de Vries, L., Oliveira, S., and van Bergen En Henegouwen, P. M. (2013) Rapid optical imaging of human breast tumour xenografts using anti-HER2 VHHs site-directly conjugated to IRDye 800CW for image-guided surgery. *Eur. J. Nucl. Med. Mol. Imaging 40*, 1718−1729.
(31) Saerens, D., Conrath, K., Govaert, J., and Muyldermans, S. (2008) Disulfide bond introduction for general stabilization of immunoglobulin heavy-chain variable domains. *J. Mol. Biol. 377*, 478−488.
(32) Govaert, J., Pellis, M., Deschacht, N., Vincke, C., Conrath, K., Muyldermans, S., and Saerens, D. (2012) Dual beneficial effect of interloop disulfide bond for single domain antibody fragments. *J. Biol. Chem. 287*, 1970−1979.
(33) Schmiedl, A., Breitling, F., Winter, C. H., Queitsch, I., and Dubel, S. (2000) Effects of unpaired cysteines on yield, solubility and activity of different recombinant antibody constructs expressed in E. coli. *J. Immunol. Methods 242*, 101−114.
(34) Stimmel, J. B., Merrill, B. M., Kuyper, L. F., Moxham, C. P., Hutchins, J. T., Fling, M. E., and Kull, F. C. (2000) Site-specific conjugation on serine → cysteine variant monoclonal antibodies. *J. Biol. Chem. 275*, 30445−30450.
(35) Eser, M., Masip, L., Kadokura, H., Georgiou, G., and Beckwith, J. (2009) Disulfide bond formation by exported glutaredoxin indicates glutathione's presence in the E. coli periplasm. *Proc. Natl. Acad. Sci. U. S. A. 106*, 1572−1577.
(36) Hermanson, G. T. (2008) *Bioconjugate techniques*, 2nd ed., Academic Press, London, U.K.
(37) Gainkam, L. O. T., Caveliers, V., Devoogdt, N., Vanhove, C., Xavier, C., Boerman, O., Muyldermans, S., Bossuyt, A., and Lahoutte, T. (2011) Localization, mechanism and reduction of renal retention of technetium-99m labeled epidermal growth factor receptor-specific nanobody in mice. *Contrast Media Mol. Imaging 6*, 85−92.
(38) Price, E. W., and Orvig, C. (2014) Matching chelators to radiometals for radiopharmaceuticals. *Chem. Soc. Rev. 43*, 260−290.
(39) Orlova, A., Rosik, D., Sandstrom, M., Lundqvist, H., Einarsson, L., and Tolmachev, V. (2007) Evaluation of In-111/114m CHX-A″-DTPA-Z(HER2:342), an Affibody ligand conjugate for targeting of HER2-expressing malignant tumors. *Quarterly Journal of Nuclear Medicine and Molecular Imaging 51*, 314−323.
(40) Conrath, K. E., Lauwereys, M., Galleni, M., Matagne, A., Frere, J. M., Kinne, J., Wyns, L., and Muyldermans, S. (2001) Beta-lactamase inhibitors derived from single-domain antibody fragments elicited in the Camelidae. *Antimicrob. Agents Chemother. 45*, 2807−2812.
(41) Chen, Z. D., and Ruffner, D. E. (1998) Amplification of closed circular DNA in vitro. *Nucleic Acids Res. 26*, 1126−1127.
(42) Vincke, C., Gutierrez, C., Wernery, U., Devoogdt, N., Hassanzadeh-Ghassabeh, G., and Muyldermans, S. (2012) Generation of single domain antibody fragments derived from camelids and generation of manifold constructs. *Methods Mol. Biol. 907*, 145−76.
(43) Gasteiger, E., Hoogland, C., Gattiker, A., Duvaud, S., Wilkins, M. R., Appel, R. D., and Bairoch, A. (2005) Protein Identification and Analysis Tools on the ExPASy Server, in *The Proteomics Protocols Handbook* (Walker, J. M., Ed.) pp 571−607, Humana Press, Totowa.
(44) D'Huyvetter, M., Aerts, A., Xavier, C., Vaneycken, I., Devoogdt, N., Gijs, M., Impens, N., Baatout, S., Ponsard, B., Muyldermans, S., Caveliers, V., and Lahoutte, T. (2012) Development of 177Lu-nanobodies for radioimmunotherapy of HER2-positive breast cancer: evaluation of different bifunctional chelators. *Contrast Media Mol. Imaging 7*, 254−264.
(45) Vanhove, C., Defrise, M., Bossuyt, A., and Lahoutte, T. (2009) Improved quantification in single-pinhole and multiple-pinhole SPECT using micro-CT information. *Eur. J. Nucl. Med. Mol. Imaging 36*, 1049−1063.